Development 140, 897-905 (2013) doi:10.1242/dev.080192
© 2013. Published by The Company of Biologists Ltd

The microRNA miR-7 regulates Tramtrack69 in a developmental switch in *Drosophila* follicle cells

Yi-Chun Huang, Laila Smith, John Poulton and Wu-Min Deng*

SUMMARY

Development in multicellular organisms includes both small incremental changes and major switches of cell differentiation and proliferation status. During *Drosophila* oogenesis, the follicular epithelial cells undergo two major developmental switches that cause global changes in the cell-cycle program. One, the switch from the endoreplication cycle to a gene-amplification phase, during which special genomic regions undergo repeated site-specific replication, is attributed to Notch downregulation, ecdysone signaling activation and upregulation of the zinc-finger protein Tramtrack69 (Ttk69). Here, we report that the microRNA miR-7 exerts an additional layer of regulation in this developmental switch by regulating Ttk69 transcripts. miR-7 recognizes the 3′ UTR of *ttk69* transcripts and regulates Ttk69 expression in a dose-dependent manner. Overexpression of miR-7 effectively blocks the switch from the endocycle to gene amplification through its regulation of *ttk69*. miR-7 and Ttk69 also coordinate other cell differentiation events, such as vitelline membrane protein expression, that lead to the formation of the mature egg. Our studies reveal the important role miR-7 plays in developmental decision-making in association with signal-transduction pathways.

KEY WORDS: MicroRNA, Follicular epithelium, Notch signaling, EcR signaling, Ttk69 (Ttk), VM32E, Gene amplification

INTRODUCTION

Precise control of DNA replication is crucial for genome stability, cell division and growth control. Most somatic cells replicate DNA once per cell cycle, to maintain the standard numbers of chromosomes and genes. In some cancerous and differentiated cells, however, this rule is broken and DNA is copied without cell division. The *Drosophila* egg chamber, the developmental unit of oogenesis, is an excellent model system in which to study how developmental signals control different DNA-replication and cell-cycle patterns (Dobens and Raftery, 2000; Klusza and Deng, 2011). During oogenesis, the somatically derived follicle cells undergo mitosis until stage 6 followed by three rounds of endocycling, during which they replicate their genomic contents without division. Finally, at stage 10B they switch into a phase known as gene amplification, during which specific genomic regions are selectively amplified (e.g. the chorion gene region); this stage is therefore referred to as the chorion gene-amplification or simply the amplification stage (Calvi et al., 1998; Cayirlioglu et al., 2001). This endocycle-to-amplification (E/A) switch, which is marked by a change from the oscillating genome-wide DNA replication pattern to a focused site-specific pattern, allows maximum production of materials required for eggshell synthesis during egg production and has served as a model system in which to determine how DNA replication origins are selected and fired (Calvi and Spradling, 1999; Tower, 2004; Claycomb and Orr-Weaver, 2005). Similar gene amplification has also been found in certain types of cancer cells; the genomic regions that contain the *Myc* gene and neighboring DNA sequence are selectively amplified (Collins and Groudine, 1982; Lee et al., 1984).

The E/A switch in main body follicle cells is triggered by two signaling events: downregulation of Notch signaling, which is normally active during endocycle stages; and activation of the hormonal ecdysone receptor (EcR) pathway. Both occur at oogenesis stage 10B and are necessary for upregulated expression of a zinc-finger protein Tramtrack 69 kDa isoform (Ttk69; Ttk – FlyBase), which also has a role in the E/A switch (Jordan et al., 2006; Sun et al., 2008; Boyle and Berg, 2009). Other factors important for DNA replication and cell-cycle regulation are required for gene amplification, such as E2F, RBF, components of the origin recognition complex, Doubleparked and epigenetic regulators (Royzman et al., 1999; Cayirlioglu et al., 2001; Cayirlioglu et al., 2003).

Changes in the cell-cycle pattern in follicle cells are strictly temporally regulated. In addition to developmental signaling pathways, a class of small regulatory RNAs, the endogenously encoded microRNA (miRNA), has also been shown to be involved in temporal regulation of cell differentiation in development. The very first mutant-miRNA phenotype observed (*lin-4* and *let-7*) was the heterochronic phenotype in the roundworm *Caenorhabditis elegans* (Reinhart et al., 2000; Grishok et al., 2001). The larval cells of these heterochronic mutants remain in the first-instar larval stage and do not progress to the second instar. Similarly, their homologs in *Drosophila* (*miR-125* and *let-7*) are involved in temporal regulation of metamorphic processes (Caygill and Johnston, 2008; Sokol et al., 2008), suggesting a conserved role for these miRNAs in temporal regulation of development. Our recent study revealed the miRNA biogenesis pathway functions in the transition from the mitotic cycle to the endocycle in the follicle cells of the fly egg chamber (Poulton et al., 2011). Here, we report that miR-7 modulates the E/A switch by acting directly on Ttk69 transcripts.

MATERIALS AND METHODS

Fly stocks and genetic clones

The following alleles were used in this study: *FRT42D miR-7*$^{\Delta 1}$ (a gift from R. W. Carthew, Northwestern University, Evanston, IL, USA), a null allele generated by excision of the *miR-7* sequence, last two exons of *bl* and two exons of *hillarin* (Li and Carthew 2005), *UAS-miR-7.140* (a gift from S. M. Cohen, Institute of Molecular and Cellular Biology, Singapore) (Stark et al., 2003), *ttk69-RNAi* (Vienna *Drosophila* RNAi Center), *UAS-Ttk69*

Department of Biological Science, Florida State University, Tallahassee, FL 32306-4295, USA.

*Author for correspondence (wumin@bio.fsu.edu)

Accepted 7 December 2012

(Bloomington Stock Center BL7361), *FRT82B ttk*^{1e11} (French et al., 2003) and *-253/-39 lacZ* (*VM32E-lacZ*) (Cavaliere et al., 2008). Notch reporters were *E(spl)mβ-CD2* (de Celis et al., 1998), *m7-lacZ* (Assa-Kunik et al., 2007) and *GbeL-lacZ* (Furriols and Bray, 2001). The following markers lines were used in clonal analysis: *FRT42D,hRFP/Cyo* (*FRT42D* recombined BL 23651); *w*^{1118}; *FRT82B,ubi-mRFP*^{nls} (BL 30555); and *w*^{1118}; *act>CD2>Gal4,UAS-RFP/TM3,Sb* (BL 30558).

Flies were maintained and raised at 25°C. FLP-out clones (mentioned as overexpression) were created with *act>CD2>Gal4,UAS-RFP/TM3,Sb*, and adult female flies were heat shocked for 30 minutes at 37°C 2-4 days before dissection. FLP/FRT mosaic clones were generated as previously described (Sun et al., 2008).

Immunocytochemistry, BrdU labeling and imaging

Immunocytochemistry and BrdU labeling were preformed as previously described (Sun and Deng, 2005) with the following antibodies: mouse anti-BrdU (1:50; BD Bioscience), rabbit anti-Ttk69 (1:200; a gift from P. Badenhorst, University of Birmingham, UK), rabbit anti-VM32E (1:100; a gift from V. Cavaliere, University of Bologna, Italy), mouse anti-CD2 (1:50; AbD Serote), rabbit anti-β-Galactosidase (1:2000; MP Biomedicals), mouse anti-β-Galactosidase (1:500; Promega), mouse anti-Cut (2B10; 1:50) and mouse anti-Hnt (1G9; 1:15; Development Studies Hybridoma Bank). Nuclei were labeled with DAPI (Invitrogen). Images were acquired with a Zeiss LSM-510 confocal microscope, and figures were prepared using Adobe Photoshop.

Expression of *hs-miR-7* in ecdysone sensor

To generate *hs-miR-7* transgenic flies, we modified primers from the original *UAS-miR-7* construct (Li and Carthew, 2005): 5′-CACGAAGAATTCGTCTAACCACCCATCCCCACAA-3′ and 5′-CAGCAATCTAGAATGGGAGGGTACTGGGGAGTTC-3′ (modified nucleotides are underlined). The PCR products were then cloned into the *Eco*RI-*Xba*I-cut pCaSpeR-hs vector (DGRC) and injected into flies.

Adult female flies of *hs-miR-7* crossed to ecdysone sensor *hs-Gal4-EcR*^{LDB}*, UAS-nlacZ*$^{7.4}$ (Kozlova and Thummel, 2002) were heat shocked for 45 minutes at 37°C for 2 days and allowed to recover at 25°C for 16 hours before dissection.

Construction of *ttk69* 3′UTR wild-type and mutated sensors

The two *ttk* isoforms have completely different 3′UTR sequences (the 69 kDa has a long UTR, the 88 kDa has a short one). miR-7 is predicted to interact with the 69 kDa isoform 3′UTR. The entire *ttk69* 3′UTR, amplified by primers 5′-GTGCGGCCGCTCTCTGGGCACCTCACACCAAG-3′ and 5′-GTCTCGAGGGAAGTTTGCCTTGCATTACGA-3′, was ligated into the *Not*I-*Xho*I-cut JB26 tub-EGFP vector (a generous gift from E. C. Lai, Memorial Sloan-Kettering Cancer Center, New York, USA) and protocols were as previously described (Silver et al., 2007).

To create a site-directed mutated sensor, we used PCR mutagenesis. The PCR was carried out with two complementary primers containing the mutant-*miR-7* target sequence: 5′-CAATCGAACCAATCTagCAAACATCTCTTT-3′ and 5′-AAAGAGATGTTTGctAGATTGGTTCGATTG-3′, and a high-fidelity *Pfu* polymerase. The PCR product was then treated with the *Dpn*I endonuclease, which digested the parental DNA template. The PCR mutagenesis result was confirmed by DNA sequencing. These resulting plasmids were then used to create transgenic flies (GenetiVision, Houston, TX, USA).

RESULTS

Overexpression of miR-7 leads to a failure to switch to the gene amplification stage

Previously, we have reported that the miRNA biogenesis pathway, including Dicer-1 and Pasha is involved in regulation of the temporal pattern of Notch signaling and the cell-cycle switches in the follicular epithelium (Poulton et al., 2011). To identify the miRNA(s) involved in this regulation, we looked at miR-7, which has been reported to regulate Notch and EGFR pathways in *Drosophila* imaginal discs and sensory organ precursors (Li et al., 2009). To determine whether miR-7 plays a role in regulating follicle cell differentiation, we overexpressed miR-7 (Stark et al., 2003) using the flip-out-GAL4 system (Pignoni and Zipursky, 1997). The normal cell-fate changes that occur in follicle cells can be revealed by staining for two transcription factors, Cut and Hindsight (Hnt), which have complementary expression patterns in follicle cells during oogenesis (Sun and Deng, 2005; Sun and Deng, 2007). Normally, Cut is expressed in early (stages 1-6) and late oogenesis (stage 10B to later), whereas Hnt is expressed only in midoogenesis (stages 7-10A), when follicle cells are undergoing endoreplication (Fig. 1A,B). When antibody markers for Cut and Hnt expression were used, no defect was detected in miR-7-overexpressing cells during the switch from the mitotic cycle to the endocycle (stages 6/7 of oogenesis). Surprisingly, miR-7 overexpression caused defects in the expression patterns of both Cut and Hnt after stage 10A, i.e. prolonged Hnt expression beyond stage 10A (98%, *n*=257 clones), whereas wild-type cells had already lost Hnt expression (Fig. 1C) and failed to express Cut protein (87%, *n*=186) (Fig. 1D), which is normally upregulated in main-body follicle cells at stage 10B. Within these miR-7 overexpression clones, we noticed that Cut expression was not at the same level from cell to cell. This variegation of Cut expression was probably caused by the variegation of the bipartite GAL4/UAS system in the follicle cell lineage (Skora and Spradling, 2010). In cells with higher levels of Gal4-induced RFP and miR-7 expression, Cut expression generally appeared lower (Fig. 1D″). Together, these results indicate that follicle-cell differentiation is disrupted when miR-7 is overexpressed during late oogenesis.

During stage 10B, the changes in cell signaling activity and gene expression culminate in the E/A switch, during which specific genomic loci are replicated repeatedly. To determine whether miR-7 overexpression resulted in a disruption of this DNA-replication-pattern change, we used bromodeoxyuridine (BrdU), a synthetic thymine analog, labeling to determine whether DNA replication was affected. In stage 10A or younger follicle cells, BrdU labeling is detected in the entire nucleus in an oscillating pattern, demonstrating that the cells are still going through periods of genome-wide replication, during either mitosis or endoreplication. After the E/A switch, the BrdU pattern takes the form of distinct foci that label only specific chromosomal loci in the wild type. In miR-7 overexpressing cells, BrdU labeled the entire nucleus in an oscillating pattern (91%, *n*=178; Fig. 1E), whereas neighboring wild-type follicle cells presented the typical pattern of foci. Taken together, these results indicate that overexpressed miR-7 can cause defects in cell fate and the E/A switch in follicle cells.

miR-7 overexpression does not affect Notch activation or EcR signaling during the E/A switch

Notch signaling downregulation is necessary for follicle cells to leave the endocycle and begin synchronous gene amplification. Forced continued activation of Notch signaling in these cells results in a failure to undergo the E/A switch, in Hnt downregulation and in Cut upregulation (Sun et al., 2008). To determine how miR-7 regulates the E/A switch in follicle cells, we first asked whether the failure to undergo the E/A switch in miR-7-overexpressing follicle cells was caused by a disturbance in Notch signaling, i.e. whether miR-7 overexpression extended Notch activity. To this end, we examined the expression of the Notch activity reporter *E(spl):CD2*, which contains the regulatory sequence of the *E(spl)* gene, a direct target of Notch intracellular domain (NICD) and its nuclear partner Supressor of hairless [Su(H)], fused to the rat *CD2* gene (de Celis et al., 1998). Normally, Notch is activated in stage 7-10A follicle cells, as

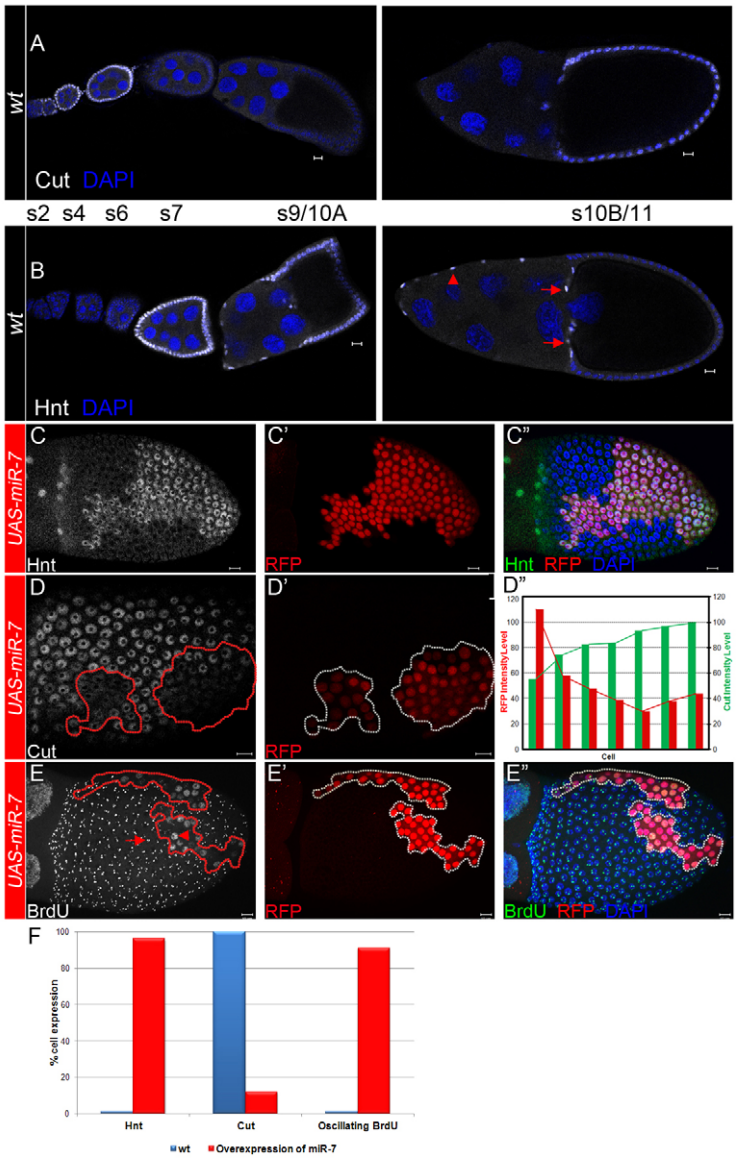

Fig. 1. Overexpression of miR-7 causes a defect in the E/A switch in follicle cells. (**A**) Expression of Cut by follicle cells in early-stage egg chambers (s1-s6). At stage 7, Notch is activated, and therefore no Cut expression is observed; these stages are called the middle stage (s7-s10A). Once Notch is downregulated at stage 10B, Cut staining reappears. (**B**) By contrast, Hnt is present only at the middle stages, when Notch is activated. At stage 10B, Hnt expression is limited to the anterior follicle cells (arrows, centripetal cells; arrowhead, stretch cells). (C-E″) In stage 10B egg chambers, follicle cells (red) with miR-7 overexpression (induced by Flp-out Gal4) are outlined with dotted lines. (**C-C″**) Prolonged Hnt staining (98%, *n*=257) was observed in cells overexpressing miR-7. (**D**,**D′**) Cells with overexpressed miR-7 failed to induce late-stage Cut expression (87%, *n*=186). (**D″**) Signaling intensity analysis of RFP and Cut expression in D. RFP intensity (*y*-axis, left) is negatively correlated with Cut expression intensity (*y*-axis, right) in miR-7-overexpressing cells (*x*-axis). (**E-E″**) Oscillating genomic BrdU incorporation (indicated by an arrowhead) was found in miR-7-overexpressing follicle cells (outlined). Neighboring wild-type cells all showed a punctate pattern (red arrow). (**F**) Quantitative analysis of Hut, Cut and BrdU, respectively, in stage 10B cells with overexpressed miR-7. DAPI (blue) was used to mark cell nuclei. Posterior is towards the right. Scale bars: 10 μm.

indicated by increased CD2 staining. If overexpression of miR-7 disrupts the E/A switch by inhibiting the downregulation of Notch signaling at stage 10B, then we would predict that CD2 levels should remain high in those cells, but that result was not observed (91% showed normal levels of CD2 expression, *n*=301; Fig. 2A). In addition, the expression of two other Notch reporters, *Gbe-lacZ* (Furriols and Bray, 2001) and *m7-lacZ* (Assa-Kunik et al., 2007), remained unchanged in follicle cells with miR-7 overexpression (data not shown), indicating that miR-7 does not regulate Notch activity [NICD/Su(H) mediated activation] in follicle cells.

In addition to Notch, our previous findings have demonstrated that the EcR pathway also regulates the E/A switch (Sun et al., 2008). Downregulation of Notch signaling allows activation of the EcR pathway at stage 10B for the E/A switch (Sun et al., 2008). An accurate reporter of EcR activity in the follicle cells at this stage is *hs-Gal4-EcR.LBD, UAS-nlacZ* (Kozlova and Thummel, 2002), which has a Gal4 DNA-binding domain fused with the EcR ligand-binding domain. The presence of ecdysone in the cell triggers the fused protein to activate *UAS-lacZ* expression. This reporter reveals uniform upregulation of *lacZ* expression at stage 10B in main-body follicle cells (Sun et al., 2008). Because this reporter also uses the Gal4/UAS system to monitor EcR activity, we generated a heat-shock-inducible construct, *hs-miR-7*, and made a transgenic fly line. Heat-shock-induced expression of miR-7 caused decreased levels of Cut in follicle cells (Fig. 2B), suggesting this transgene behaves in a similar way to the aforementioned *UAS-miR-7* during the E/A switch. However, no significant difference in β-Galactosidase antibody staining was detected (Fig. 2B′), indicating normal EcR activity in these cells. To confirm this result, we also used an *EcRE-lacZ* reporter (BL 4516), which contains the ecdysone-responsive element upstream of the *lacZ* reporter gene. Its expression is normally detected in all follicle cells after stage 9. miR-7 overexpression did not change the pattern of this reporter either (data not shown). These results indicate that miR-7 does not appear able to regulate ecdysone activity when overexpressed; the phenotypes associated with miR-7 overexpression in follicle cells are therefore probably not a result of altered EcR signaling.

miR-7 regulates Ttk69 expression dose dependently during the E/A switch

Because neither Notch nor EcR pathways appear to be the target of miR-7 in follicle cells during the E/A switch, we turned our attention

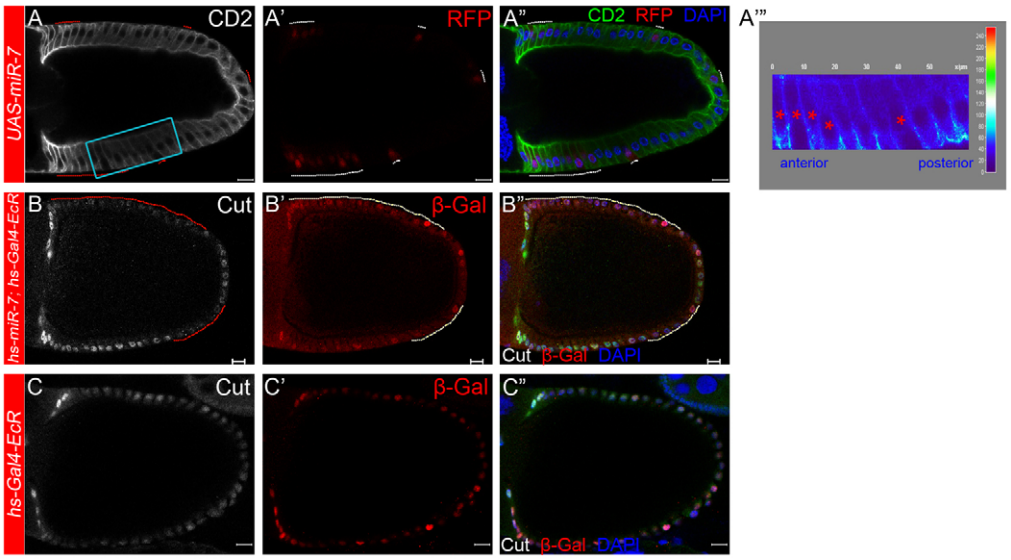

Fig. 2. miR-7 does not regulate Notch or ecdysone signaling during the E/A switch. (**A-A‴**) Notch activation is marked with E(Spl)-CD2 expression. No increased CD2 staining (white in A and green in A″) was observed in stage 10B follicle cells with overexpressed miR-7 (red in A′ and A″). (A‴) Intensity analysis representing the CD2 expression level of the blue-boxed area in A (clone cells marked with asterisks). (Plot was generated using ImageJ v1.46j interactive 3D surface plot.) miR-7 overexpression was induced by flip-out *Gal4* driven *UAS-miR-7*, and marked with β-Galactosidase expression (red) (**B-B″**) Follicle cells with heat shock-induced overexpression of miR-7 (*hs-miR-7*) were revealed by Cut downregulation (white in B, outlined). In this stage 10B egg chamber, no clear difference was detected between miR-7-overexprssing cells and neighboring wild-type cells in ecdysone signaling activity, as revealed by β-Galactosidase staining (red in B′ and B″) of the *hs-Gal4-EcR; UAS-LZ* reporter. (**C-C″**) In a control experiment without *hs-miR-7*, the patched β-Galactosidase staining (red in C′ and C″) did not have any effect on the Cut expression (C). DAPI (blue) was used to mark cell nuclei. Posterior is towards the right. Scale bars: 10 μm.

to Ttk69, a zinc-finger protein isoform whose upregulation is required for the E/A switch (Sun et al., 2008). In normal developing egg chambers, Ttk69 is expressed in follicle cells at low levels, from the germarium until stage 10A (Fig. 3A); at stage 10B, in response to high levels of ecdysone signaling, Ttk69 levels sharply increase (Fig. 3A) (Sun et al., 2008). Manipulation of Ttk69 expression levels during the E/A switch also affects the expression of Cut and Hnt (Sun et al., 2008). To test the possibility that miR-7 affects the E/A switch by regulating Ttk69 levels, we measured Ttk69 expression in follicle cells overexpressing miR-7. In stage 10B cells overexpressing miR-7, Ttk69 expression was lower than in wild-type neighboring cells (87%, n=306; Fig. 3B), suggesting miR-7 can regulate Ttk69 expression levels during the E/A switch.

To determine whether miR-7 endogenously regulates Ttk69 expression in follicle cells, we performed a loss-of-function analysis using the FLP-FRT technique and a *miR-7* null allele, *miR-7*$^{\Delta 1}$ (Li and Carthew, 2005). In stage 10A *miR-7*$^{\Delta 1}$ follicle-cell clones, Ttk69 expression was elevated earlier than that in its wild-type neighbors (83%, n=415; Fig. 3C). Interestingly, we found that this phenomenon was dependent on the dose of miR-7. In homozygous RFP follicle cells, called twin-spot cells, which are generated during the FLP-FRT-induced recombination resulting in mutant follicle cells, we observed the lowest Ttk69 level (Fig. 3D). Heterozygous cells with one copy of *miR-7*$^{\Delta 1}$ and one copy of the wild-type gene had intermediate levels of Ttk69, whereas homozygous mutant *miR-7*$^{\Delta 1}$ clones showed the highest Ttk69 expression (Fig. 3D). These results indicate that miR-7 regulates Ttk69 levels in a dose-dependent manner in follicle cells during the E/A switch.

Direct regulation of Ttk69 by miR-7

Because Ttk69 expression levels were sensitive to changes in the copy number of the *miR-7* gene, we asked whether Ttk69 transcripts are directly regulated by miR-7. In support of this hypothesis, bioinformatic analysis with the 'TargetScanFly' (Ruby et al., 2007) and 'miRanda' (Betel et al., 2008) programs indicated that the *ttk69* 3′UTR has a single predicted miR-7 recognition site. To verify whether *ttk69* is a direct target of miR-7, we constructed a sensor line containing GFP expressed under the *tubulin* promoter followed by the 3′UTR sequence of *ttk69*. In the wild-type background, the expression of this GFP sensor was hardly detectable. If the *ttk69* 3′UTR contains the miR-7 target site, then loss of *miR-7* should lead to derepression of the *ttk69* 3′UTR sensor, and we should observe increased GFP signal (supplementary material Fig. S1). We therefore introduced this *ttk69* 3′UTR sensor line into the *miR-7* loss-of-function background. Consistent with the hypothesis that *ttk69* is a target of miR-7, we observed strong GFP signal in *miR-7*$^{\Delta 1}$ follicle-cell clones, whereas wild-type neighbor cells lacked GFP expression (Fig. 4A). To verify that *ttk69* is a direct target of miR-7, we also generated a mutated *ttk69* 3′UTR sensor with the miR-7 target sequence TCTTCCA mutated to TCTagCA (supplementary material Fig. S1). As expected, expressing this mutated *ttk69* 3′UTR sensor in the *miR-7* loss-of-function background produced no difference in GFP expression in clone cells and wild-type neighbor cells (Fig. 4B). These data strongly suggest that miR-7 directly regulates Ttk69 expression through the single miR-7 target site at the *ttk69* 3′UTR.

To determine whether the regulation of Ttk69 levels is important to *miR-7*-induced phenotypes in follicle cells, we co-expressed miR-7 and Ttk69 in follicle cells and examined Cut and Hnt expression levels. To avoid repression of misexpressed Ttk69 by miR-7, we used a *UAS-Ttk69* transgene constructed from *ttk69* cDNA without the 3′UTR and thus lacking the miR-7 binding site. If miR-7 regulates the E/A switch by controlling *ttk69* transcripts,

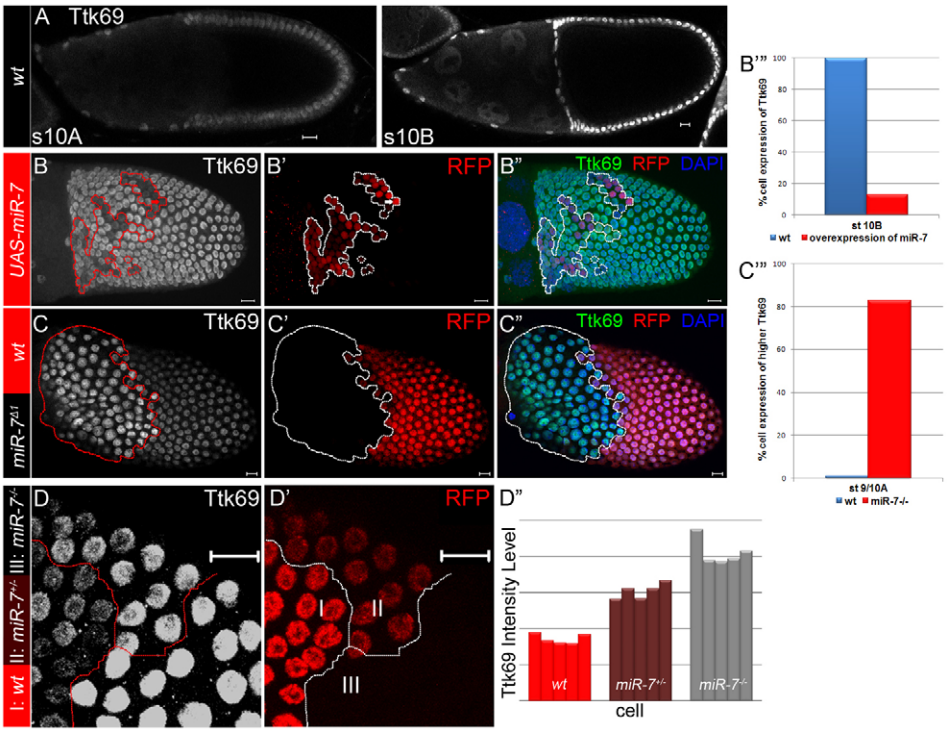

Fig. 3. Regulation of Ttk69 expression by miR-7. (**A**) Expression of Ttk69 at low levels during oogenesis through stage 10A. At stage 10B, Ttk69 is upregulated in the main-body follicle cells. (**B-B″**) Collapsed images of the *z*-stacks. Lower Ttk69 expression in cells overexpressing miR-7 (red) than in wild-type neighbors. Arrow indicates brighter RFP, i.e. a higher amount of miR-7 was expressed and stronger repression of Ttk69. (**B‴**) Quantitative analysis of Ttk69 levels in stage 10B cells with overexpressed miR-7. (**C-C″**) FLP/FRT *miR-7*$^{\Delta 1}$ clone cells (outlined, absence of red), revealing earlier Ttk69 upregulation than in adjacent cells. (**C‴**) Quantitative results of higher Ttk69 expression at stage 9/10A *miR-7*$^{-/-}$ clone cells. (**D**,**D′**) Higher magnification and collapsed images of the *z*-stacks. The Ttk69 signaling level depends on miR-7 dose. The homozygous RFP follicle cells (area I) had the lowest Ttk69 staining, whereas homozygous mutant *miR-7* $^{\Delta 1}$ clones showed the highest Ttk69 expression (absence of red, area III). (**D″**) Intensity analysis of Ttk69 expression levels (*y*-axis) in D. Five cells were randomly selected from each of the three areas marked in D′ and grouped together. DAPI (blue) was used to mark cell nuclei. Posterior is towards the right. Scale bars: 10 μm.

with extra Ttk69 present in miR-7-overexpressing follicle cells, we should not observe downregulated Cut and prolonged Hnt phenotypes. Indeed, we found that the Cut downregulation phenotype was alleviated (96%, *n*=104; Fig. 4C), and in some cases we were able to find slightly increased Cut (Fig. 4C, arrows). Similarly, the increased levels of Hnt we observed at stage 10B in response to miR-7 overexpression alone were no longer present when we co-expressed Ttk69 (95%, *n*=228; Fig. 4D). In addition, the BrdU labeling showed the typical focal pattern in clone cells with co-expression of Ttk69 and miR-7 (89%, *n*=107; Fig. 4E), indicating that these cells enter the gene amplification cycle similar to their wild-type neighbors.

Loss of *miR-7* is not sufficient to activate premature E/A switch

Overexpression of miR-7 can disrupt the E/A switch, and expression of markers such as Hnt and Cut suggests that miR-7 plays a role in regulating these processes. Furthermore, we have demonstrated that miR-7 does repress Ttk69 (Fig. 3B), and increased Ttk69 levels are important in promoting the E/A transition (Sun et al., 2008). We therefore asked whether loss of *miR-7* would lead to a premature E/A switch owing to the increased Ttk69 expression. In *miR-7* mutant clones, we detected no premature E/A switch, as revealed by a focal pattern of BrdU incorporation (Fig. 5). We also only rarely observed increased Hnt in stage 10A egg chambers, and we detected no early Cut downregulation (data not shown). We conclude that, although loss of *miR-7* is sufficient to cause early Ttk69 upregulation, it is not sufficient to drive the E/A switch, suggesting additional developmental factors are required to trigger this transition.

miR-7 and Ttk69 regulate vitelline membrane gene expression

During the late stages of oogenesis, many changes take place in the follicle cells in preparation for egg maturation. In addition to eggshell synthesis, in which chorion-gene amplification is an important step, vitelline membrane synthesis begins at a stage slightly before gene amplification occurs. We asked whether *miR-7* and Ttk69 are involved in these developmental changes in follicle cells that lead to egg maturation, and whether they act in ways similar to those used in their control of the E/A switch. To this end, we studied the expression of a vitelline membrane protein, VM32E (Bernardi et al., 2009), in egg chambers with genetic manipulations of *miR-7* and/or *ttk69*. An antibody against VM32E revealed no expression in early oogenesis (Fig. 6A; supplementary material Fig. S2); starting at stage 9, low levels of VM32E was detected, mostly at the apical side of the follicle cells (Fig. 6A; supplementary material Fig. S2). At stages 10A and 10B, VM32E protein was readily detected in follicle cells and in the extracellular space between follicle cells and the oocyte (Fig. 6A; supplementary material Fig. S2). The distribution patterns on the apical and basal surfaces differ; on the apical side, VM32E shows a more

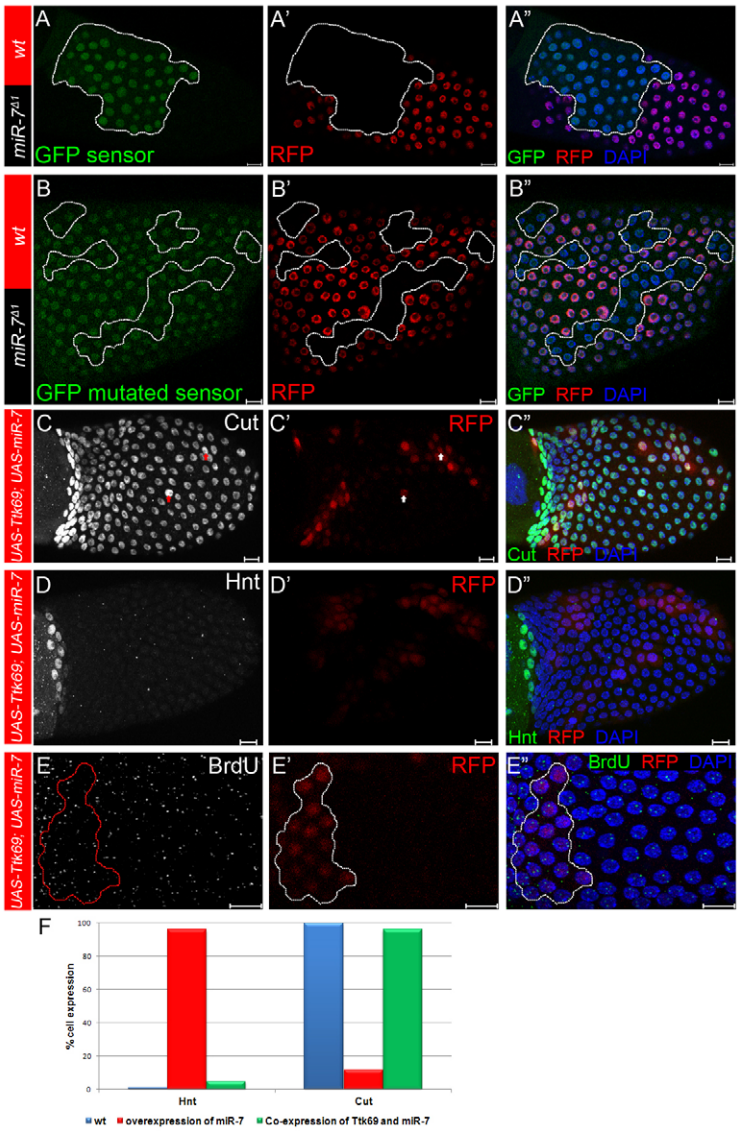

Fig. 4. Direct regulation of Ttk69 by miR-7. (A-B″) *miR-7*$^{\Delta 1}$ clone cells (absence of red, outlined). (**A-A″**) Strong GFP signal from the *ttk69* 3′UTR sensor line in clone cells; GFP was absent in wild-type neighbor cells. (**B-B″**) GFP from the mutated 3′UTR sensor line was expressed in both the *miR-7*$^{\Delta 1}$ clone (outlined) and wild-type follicle cells. (**C-C″**) Overexpression of Ttk69 rescued the decreased Cut caused by overexpression of miR-7 (compare with Fig. 1D-D″); we occasionally observed higher Cut levels in these cells (arrows). (**D-D″**) Lack of prolonged Hnt staining in the co-expression of Ttk69 and miR-7 cells. (**E-E″**) Punctate BrdU labeling was restored when Ttk69 was co-expressed with miR-7 (outlined). (**F**) Quantification of extra *Ttk69* expression needed to rescue the Hnt and Cut phenotypes in stage 10B cells with overexpressed miR-7. DAPI (blue) was used to mark cell nuclei. Posterior is towards the right. Scale bars: 10 μm.

continuous pattern, but on the basal side and the cytoplasm, it shows punctate staining (supplementary material Fig. S2). We did not observe VM32E expression in the anterior columnar follicle cells, the centripetal cells, or the posterior follicle cells (Fig. 6A). To determine the relationship between *miR-7* and VM32E expression, we examined the levels of VM32E protein in response to overexpression or deletion of *miR-7*. Overexpression of miR-7 resulted in loss of VM32E expression after stage 10 [Fig. 6B; supplementary material Fig. S3; 83% (*n*=97) during stages 9/10A and 91% (*n*=171) at stage 10B], whereas in mutant *miR-7* clones, we found increased VM32E [Fig. 6C; supplementary material Fig. S4; 60% (*n*=143) during stages 9/10A and 36% (*n*=178) at stage 10B]. At the apical side, VM32E protein appeared to be able to diffuse to cover the adjacent wild-type cell (supplementary material Fig. S4, arrowhead). To determine whether miR-7 affected VM32E expression at the transcriptional or post-transcriptional level, we expressed a reporter of VM32E gene expression, *-253/-39 lacZ* (Bernardi et al., 2009), in egg chambers overexpressing *miR-7*. This transgenic line bears the -253/-39 region of the VM32E promoter and is fused to a *lacZ* reporter gene. The *-253/-39 lacZ* shows a patchy expression pattern in follicular epithelium. In cells overexpressing miR-7, we observed downregulation of β-Gal (data not shown). These results, together with the fact that no miR-7 target site was predicted at the 3′UTR of VM32E mRNA, indicate that miR-7 indirectly regulates VM32E expression in follicle cells.

Because the above results suggest that miR-7 affects both Ttk69 and VM32E expression, we asked whether Ttk69 has an effect on VM32E expression. Indeed, in follicle cells overexpressing Ttk69, we observed weak upregulation of VM32E (67.3%, *n*=447; Fig. 6D). Conversely, we found decreased VM32E both in clones

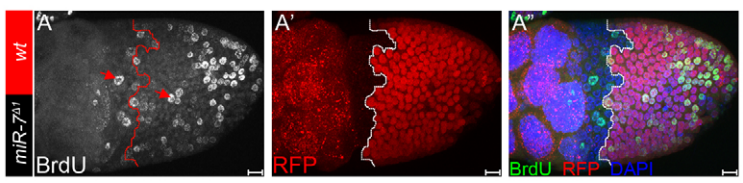

Fig. 5. Loss of *miR-7* is not sufficient to activate premature E/A switch. (**A-A″**) Oscillating genomic BrdU incorporation (arrows) can be observed in *miR-7*$^{\Delta 1}$ follicle-cell clones (absence of red) and in wild-type cells. DAPI (blue) was used to mark cell nuclei. Posterior is towards the right. Scale bars: 10 μm.

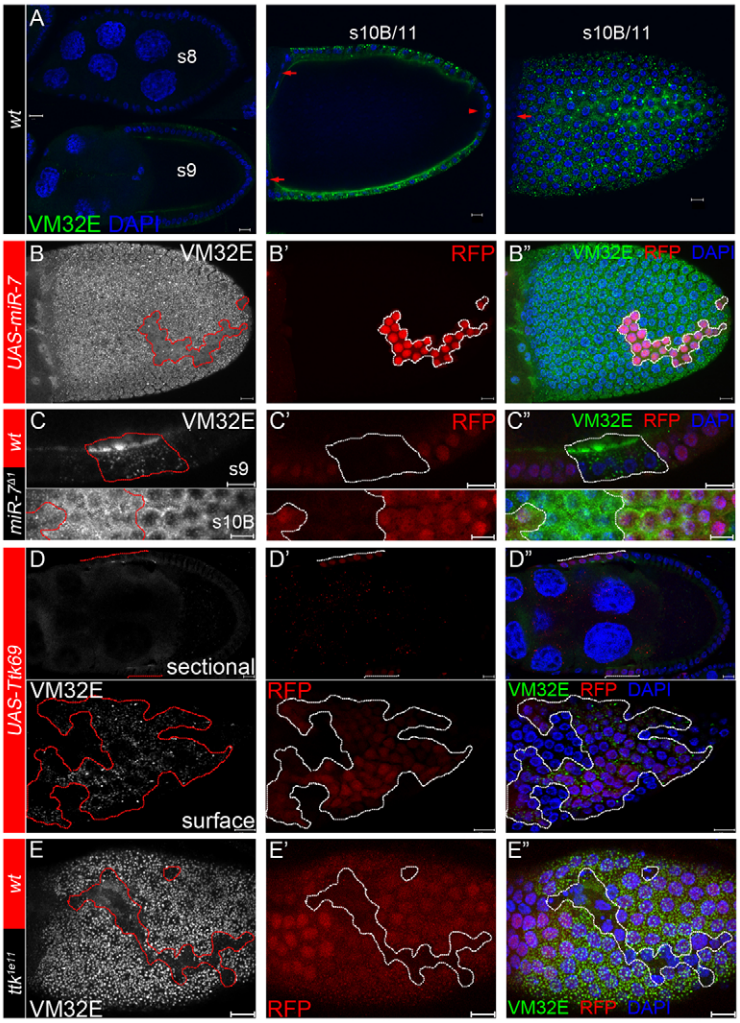

Fig. 6. Regulation of VM32E expression by miR-7. (**A**) Lack of expression of VM32E, the vitelline membrane gene, in early oogenesis. Low levels of VM32E (green) are expressed in late stage 9 egg chambers, and VM32E is then diffused into the extracellular space around the oocyte at stage 10. Centripetal cells (arrows) and posterior follicle cells (arrowhead) do not express VM32E. (**B-B″**) Suppression of VM32E by miR-7 overexpression (red, outlined). (**C-C″**) Mutant *miR-7*$^{\Delta 1}$ clones (absence of RFP, outlined) induced early upregulation of VM32E in stage 9 egg chambers and higher VM32E levels in late stage egg chambers relative to wild-type cells (RFP positive). (**D-D″**) Sectional and surface views of follicular epithelia with mild upregulation of VM32E in cells overexpressing Ttk69 (red, outlined). (**E-E″**) Decreased VM32E levels in *ttk*^{1e11} clone cells (absence of red, outlined). DAPI (blue) was used to mark cell nuclei. Posterior is towards the right. (B,E) Collapsed confocal-image stacks of two stage 10B egg chambers; the sectional images used to project these two collapsed images are shown in supplementary material Figs S3 and S5, respectively. Scale bars: 10 μm.

in which Ttk69 was knocked down by RNAi (data not shown) and in mutant *ttk69* clones (Fig. 6E; supplementary material Fig. S5). These results indicate that Ttk69 is necessary and sufficient to promote VM32E expression.

Because genetic manipulations of *miR-7* or *ttk69* resulted in altered levels of VM32E expression, we asked whether VM32E regulation by miR-7 is mediated by Ttk69. To examine this possibility, we used the mosaic analysis with a repressible cell marker (MARCM) technique to misexpress *ttk-RNAi* in *miR-7*$^{\Delta 1}$ follicle cell clones (Lee and Luo, 2001). If miR-7 regulates VM32E levels by repressing Ttk69, then downregulation of Ttk69 in *miR-7* mutant cells should lead to decreased VM32E, as we observed under *ttk69* knockdown alone. Indeed, in *miR-7* and *ttk69* double loss-of-function cells generated by the MARCM technique, VM32E expression was suppressed (82.3%, n=138; Fig. 7A,B). These findings suggest that Ttk69 acts downstream of miR-7 to promote VM32E expression.

DISCUSSION

The follicular epithelium, with two clear global changes in cell-cycle programs and differentiation status, has served as an excellent model in the study of developmental switches (reviewed by Klusza and Deng, 2011). The rise and fall (activation and downregulation) of Notch signaling in the follicle cells have direct effects on the two developmental switches. miRNAs, however, play important modulatory roles in controlling the timing of these two switches (Poulton et al., 2011; this study), but clear differences exist. During the mitotic-to-endocycle switch, the miRNAs directly regulate the

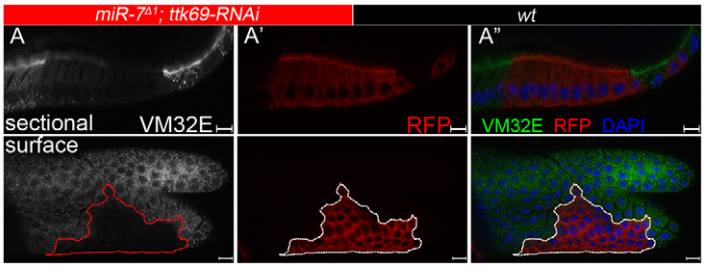

Fig. 7. miR-7 regulates VM32E through Ttk69. (**A-A″**) Reduced VM32E (white in A and green in A″) expression was detected in *miR-7*$^{\Delta 1}$ MARCM clones (outlined and marked by RFP, red) with *ttk69-RNAi* expression in this stage 11 egg chamber (top, sectional views; bottom, surface views). Posterior is towards the right. DAPI (blue) was used to mark cell nuclei in A″. Scale bars: 10 μm.

timing of Notch activation by acting on *cis*-expressed Delta (Poulton et al., 2011). During the E/A switch, the miRNA miR-7, does not seem to have a direct role in regulating Notch activity; instead, it acts directly on the transcription factor Ttk69, which is also a target of Notch and EcR signaling in this process.

The phenotypes of loss- and gain-of-function of *miR-7* during the E/A switch can be explained by its direct regulation of Ttk69. *ttk69* loss-of-function (Sun et al., 2008) and miR-7 overexpression follicle cell clones both exhibit the following phenotypes: failure to switch from endocycling to gene amplification; continued Hnt expression; and lack of Cut upregulation. By contrast, loss-of *miR-7* (which induces Ttk69 upregulation) or forced overexpression of Ttk69 (Sun et al., 2008) could not shift the E/A switch earlier. Similarly, in the regulation of vitelline membrane synthesis, genetic epistatic analysis of *miR-7* and *ttk69* suggests that Ttk69 mediates the function of miR-7 in these late-staged follicle cells. Loss of *miR-7* function can actually shift VM32E expression earlier during the transitional stage and upregulate VM32E at a later stage, which is consistent with the phenotypes of Ttk69 overexpression. The impact of this misregulation on the function of the egg remains to be determined.

In the follicle cells, the change in expression of *Ttk69* in response to miR-7 levels is striking, even the heterozygous *miR-7* mutant follicle cells showed upregulated *Ttk69* expression, suggesting a dose-dependent regulation by miR-7. Intriguingly, only one miR-7 recognition site was found in the 3′UTR of the Ttk69 transcript, and this site is sufficient to mediate the repression of its expression in follicle cells by miR-7. In the eye imaginal disc, Yan, a transcription factor essential for the development of photoreceptor cells, is a direct target of miR-7 (Li et al., 2009). In that feed-forward regulatory loop, Ttk69 was indirectly regulated by miR-7. We considered the possible role of Yan in follicle cells, but clonal analysis of *yan* mutations did not generate any defect during the E/A switch (data not shown), suggesting Yan is not a relevant target in follicle cells. Therefore, the *miR-7* function depends strongly on the cellular context in which it is expressed. Intriguingly, the level of miR-7 expression in the ovary is low when compared with other miRNAs (supplementary material Fig. S6) (Berezikov et al., 2011). When a *miR-7* reporter was used to examine its expression in follicle cells (Stark et al., 2003), no obvious signal was detected (data not shown). As such a low level of miR-7 can modulate important developmental processes in follicle cells, the efficiency of miRNA use must be very high.

miRNAs have been found to be involved in important aspects of animal and plant development (Bushati and Cohen, 2007; Carlsbecker et al., 2010), as well as in a variety of human diseases, including cancer and cardiovascular diseases (Stefani, 2007; Liu and Olson, 2010). Many of their targets are transcription factors, which themselves have a broad range of target genes; this type of regulation allows miRNAs to have a more global effect in influencing cell-fate changes and other cellular events. Our studies of the involvement of miRNAs in temporal regulation in follicle cell development reveals the collaborative effect of miRNAs, signaling pathways and transcription factors in developmental decision making. In this system, transcription factor Ttk69 emerges as a common target and plays a crucial role in coordinating the effects of the miRNA and signaling pathways.

Acknowledgements
We thank Anne Thistle for reading the manuscript; Sarah Bray, Richard Carthew, Steve Cohen, Jamila Horabin, Eric Lai, the Developmental Studies Hybridoma Bank, Vienna Drosophila RNAi Center (VDRC) and Bloomington Drosophila Stock Center (BDSC) for antibodies, vectors and fly stocks; K. Riddle (FSU Imaging Laboratory); A. Irsigler, C. Pye and R. Dhanarajan (FSU Molecular Core Facility); and Michelle Arbeitman, Jamila Horabin, Daniel Vera and Gengqiang Xie for small RNA-Seq analysis.

Funding
J.S.P. was supported by an American Heart Association Predoctoral Fellowship, a National Institutes of Health (NIH) Postdoctoral Fellowship at the Lineberger Comprehensive Cancer Center [T32CA009156], and is currently supported by an NIH Fellowship [F32GM095127-01]. W.-M.D. is supported by the NIH [R01GM072562] and National Science Foundation [IOS-1052333]. Deposited in PMC for release after 12 months.

Competing interests statement
The authors declare no competing financial interests.

Supplementary material
Supplementary material available online at
http://dev.biologists.org/lookup/suppl/doi:10.1242/dev.080192/-/DC1

References
Assa-Kunik, E., Torres, I. L., Schejter, E. D., Johnston, D. S. and Shilo, B. Z. (2007). Drosophila follicle cells are patterned by multiple levels of Notch signaling and antagonism between the Notch and JAK/STAT pathways. *Development* **134**, 1161-1169.

Berezikov, E., Robine, N., Samsonova, A., Westholm, J. O., Naqvi, A., Hung, J. H., Okamura, K., Dai, Q., Bortolamiol-Becet, D., Martin, R. et al. (2011). Deep annotation of Drosophila melanogaster microRNAs yields insights into their processing, modification, and emergence. *Genome Res.* **21**, 203-215.

Bernardi, F., Romani, P., Tzertzinis, G., Gargiulo, G. and Cavaliere, V. (2009). EcR-B1 and Usp nuclear hormone receptors regulate expression of the VM32E eggshell gene during Drosophila oogenesis. *Dev. Biol.* **328**, 541-551.

Betel, D., Wilson, M., Gabow, A., Marks, D. S. and Sander, C. (2008). The microRNA.org resource: targets and expression. *Nucleic Acids Res.* **36**, D149-D153.

Boyle, M. J. and Berg, C. A. (2009). Control in time and space: Tramtrack69 cooperates with Notch and Ecdysone to repress ectopic fate and shape changes during Drosophila egg chamber maturation. *Development* **136**, 4187-4197.

Bushati, N. and Cohen, S. M. (2007). microRNA functions. *Annu. Rev. Cell Dev. Biol.* **23**, 175-205.

Calvi, B. R. and Spradling, A. C. (1999). Chorion gene amplification in Drosophila: A model for metazoan origins of DNA replication and S-phase control. *Methods* **18**, 407-417.

Calvi, B. R., Lilly, M. A. and Spradling, A. C. (1998). Cell cycle control of chorion gene amplification. *Genes Dev.* **12**, 734-744.

Carlsbecker, A., Lee, J. Y., Roberts, C. J., Dettmer, J., Lehesranta, S., Zhou, J., Lindgren, O., Moreno-Risueno, M. A., Vatén, A., Thitamadee, S. et al. (2010). Cell signalling by microRNA165/6 directs gene dose-dependent root cell fate. *Nature* **465**, 316-321.

Cavaliere, V., Bernardi, F., Romani, P., Duchi, S. and Gargiulo, G. (2008). Building up the Drosophila eggshell: first of all the eggshell genes must be transcribed. *Dev. Dyn.* **237**, 2061-2072.

Caygill, E. E. and Johnston, L. A. (2008). Temporal regulation of metamorphic processes in Drosophila by the let-7 and miR-125 heterochronic microRNAs. *Curr. Biol.* **18**, 943-950.

Cayirlioglu, P., Bonnette, P. C., Dickson, M. R. and Duronio, R. J. (2001). Drosophila E2f2 promotes the conversion from genomic DNA replication to gene amplification in ovarian follicle cells. *Development* **128**, 5085-5098.

Cayirlioglu, P., Ward, W. O., Silver Key, S. C. and Duronio, R. J. (2003). Transcriptional repressor functions of Drosophila E2F1 and E2F2 cooperate to inhibit genomic DNA synthesis in ovarian follicle cells. *Mol. Cell. Biol.* **23**, 2123-2134.

Claycomb, J. M. and Orr-Weaver, T. L. (2005). Developmental gene amplification: insights into DNA replication and gene expression. *Trends Genet.* **21**, 149-162.

Collins, S. and Groudine, M. (1982). Amplification of endogenous myc-related DNA sequences in a human myeloid leukaemia cell line. *Nature* **298**, 679-681.

de Celis, J. F., Tyler, D. M., de Celis, J. and Bray, S. J. (1998). Notch signalling mediates segmentation of the Drosophila leg. *Development* **125**, 4617-4626.

Dobens, L. L. and Raftery, L. A. (2000). Integration of epithelial patterning and morphogenesis in Drosophila ovarian follicle cells. *Dev. Dyn.* **218**, 80-93.

French, R. L., Cosand, K. A. and Berg, C. A. (2003). The Drosophila female sterile mutation twin peaks is a novel allele of tramtrack and reveals a requirement for Ttk69 in epithelial morphogenesis. *Dev. Biol.* **253**, 18-35.

Furriols, M. and Bray, S. (2001). A model Notch response element detects Suppressor of Hairless-dependent molecular switch. *Curr. Biol.* **11**, 60-64.

Grishok, A., Pasquinelli, A. E., Conte, D., Li, N., Parrish, S., Ha, I., Baillie, D. L., Fire, A., Ruvkun, G. and Mello, C. C. (2001). Genes and mechanisms

related to RNA interference regulate expression of the small temporal RNAs that control C. elegans developmental timing. *Cell* **106**, 23-34.
Jordan, K. C., Schaeffer, V., Fischer, K. A., Gray, E. E. and Ruohola-Baker, H. (2006). Notch signaling through tramtrack bypasses the mitosis promoting activity of the JNK pathway in the mitotic-to-endocycle transition of Drosophila follicle cells. *BMC Dev. Biol.* **6**, 16.
Klusza, S. and Deng, W. M. (2011). At the crossroads of differentiation and proliferation: precise control of cell-cycle changes by multiple signaling pathways in Drosophila follicle cells. *Bioessays* **33**, 124-134.
Kozlova, T. and Thummel, C. S. (2002). Spatial patterns of ecdysteroid receptor activation during the onset of Drosophila metamorphosis. *Development* **129**, 1739-1750.
Langmead, B. and Salzberg, S. L. (2012). Fast gapped-read alignment with Bowtie 2. *Nat. Methods* **9**, 357-359.
Lee, T. and Luo, L. (2001). Mosaic analysis with a repressible cell marker (MARCM) for Drosophila neural development. *Trends Neurosci.* **24**, 251-254.
Lee, W. H., Murphree, A. L. and Benedict, W. F. (1984). Expression and amplification of the N-myc gene in primary retinoblastoma. *Nature* **309**, 458-460.
Li, X. and Carthew, R. W. (2005). A microRNA mediates EGF receptor signaling and promotes photoreceptor differentiation in the Drosophila eye. *Cell* **123**, 1267-1277.
Li, X., Cassidy, J. J., Reinke, C. A., Fischboeck, S. and Carthew, R. W. (2009). A microRNA imparts robustness against environmental fluctuation during development. *Cell* **137**, 273-282.
Liu, N. and Olson, E. N. (2010). MicroRNA regulatory networks in cardiovascular development. *Dev. Cell* **18**, 510-525.
McQuilton, P., St Pierre, S. E., Thurmond, J. and the FlyBase Consortium (2012). FlyBase 101 – the basics of navigating FlyBase. *Nucleic Acids Res.* **40**, D706-D714.
Pignoni, F. and Zipursky, S. L. (1997). Induction of Drosophila eye development by decapentaplegic. *Development* **124**, 271-278.
Poulton, J. S., Huang, Y. C., Smith, L., Sun, J. J., Leake, N., Schleede, J., Stevens, L. M. and Deng, W. M. (2011). The microRNA pathway regulates the temporal pattern of Notch signaling in Drosophila follicle cells. *Development* **138**, 1737-1745.
Quinlan, A. R. and Hall, I. M. (2010). BEDTools: a flexible suite of utilities for comparing genomic features. *Bioinformatics* **26**, 841-842.
Reinhart, B. J., Slack, F. J., Basson, M., Pasquinelli, A. E., Bettinger, J. C., Rougvie, A. E., Horvitz, H. R. and Ruvkun, G. (2000). The 21-nucleotide let-7 RNA regulates developmental timing in Caenorhabditis elegans. *Nature* **403**, 901-906.
Royzman, I., Austin, R. J., Bosco, G., Bell, S. P. and Orr-Weaver, T. L. (1999). ORC localization in Drosophila follicle cells and the effects of mutations in dE2F and dDP. *Genes Dev.* **13**, 827-840.
Ruby, J. G., Stark, A., Johnston, W. K., Kellis, M., Bartel, D. P. and Lai, E. C. (2007). Evolution, biogenesis, expression, and target predictions of a substantially expanded set of Drosophila microRNAs. *Genome Res.* **17**, 1850-1864.
Silver, S. J., Hagen, J. W., Okamura, K., Perrimon, N. and Lai, E. C. (2007). Functional screening identifies miR-315 as a potent activator of Wingless signaling. *Proc. Natl. Acad. Sci. USA* **104**, 18151-18156.
Sokol, N. S., Xu, P., Jan, Y. N. and Ambros, V. (2008). Drosophila let-7 microRNA is required for remodeling of the neuromusculature during metamorphosis. *Genes Dev.* **22**, 1591-1596.
Stark, A., Brennecke, J., Russell, R. B. and Cohen, S. M. (2003). Identification of *Drosophila* microRNA targets. *PLoS Biol.* **1**, E60.
Stefani, G. (2007). Roles of microRNAs and their targets in cancer. *Expert Opin. Biol. Ther.* **7**, 1833-1840.
Sun, J. and Deng, W. M. (2005). Notch-dependent downregulation of the homeodomain gene cut is required for the mitotic cycle/endocycle switch and cell differentiation in Drosophila follicle cells. *Development* **132**, 4299-4308.
Sun, J. and Deng, W. M. (2007). Hindsight mediates the role of notch in suppressing hedgehog signaling and cell proliferation. *Dev. Cell* **12**, 431-442.
Sun, J., Smith, L., Armento, A. and Deng, W. M. (2008). Regulation of the endocycle/gene amplification switch by Notch and ecdysone signaling. *J. Cell Biol.* **182**, 885-896.
Tower, J. (2004). Developmental gene amplification and origin regulation. *Annu. Rev. Genet.* **38**, 273-304.

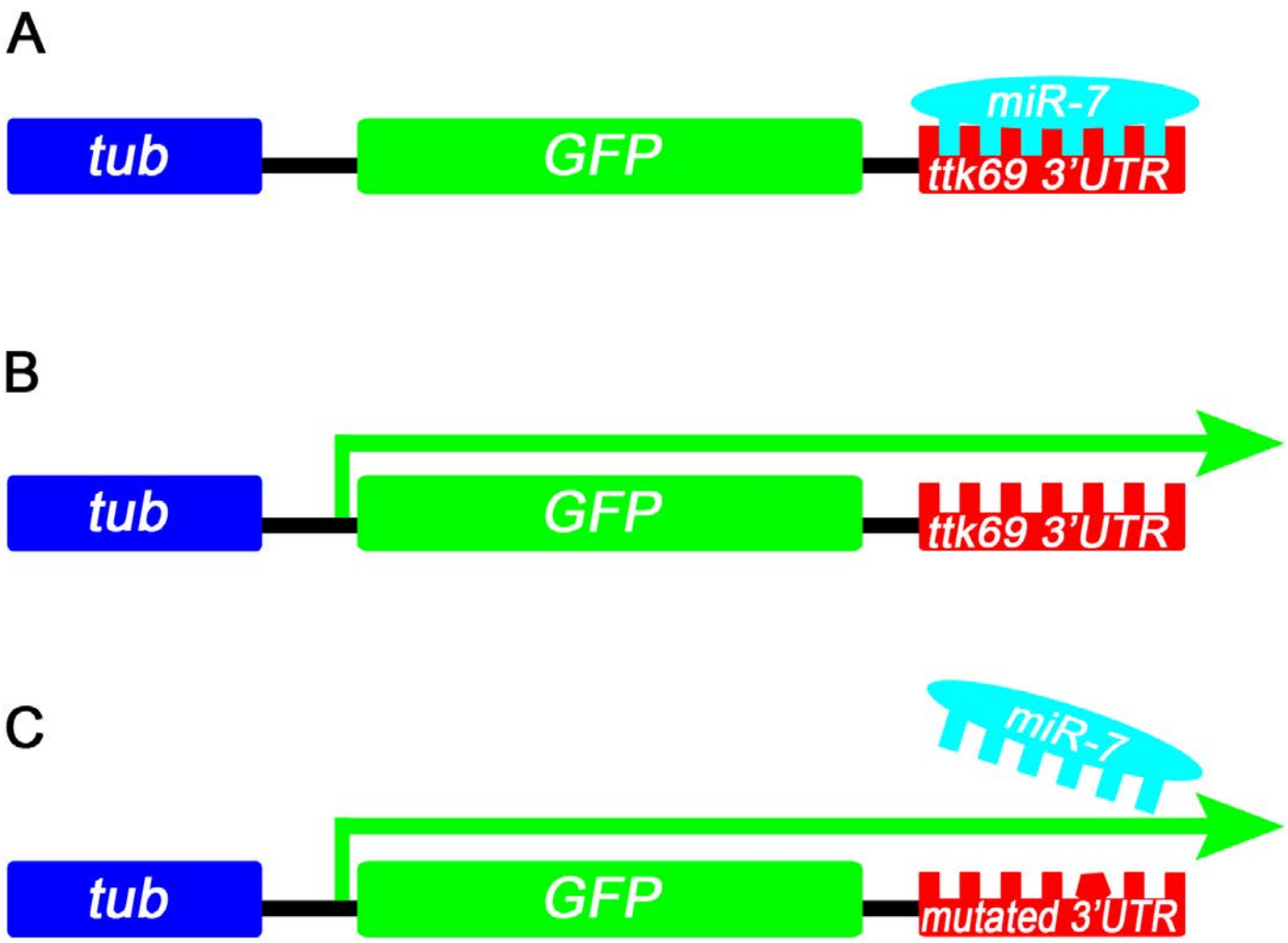

Fig. S1. The *ttk69* 3′UTR sensor, which contains a tubulin promoter, a GFP open reading frame and *ttk69* 3′ UTR. (**A**) In the wild type, miR-7 binds to the target sequence at the *ttk69* 3′UTR and represses GFP expression. (**B**) Without *miR-7*, GFP expression is derepressed. (**C**) miR-7 cannot bind to the mutated target sequence at the *ttk69* 3′UTR to repress GFP expression.

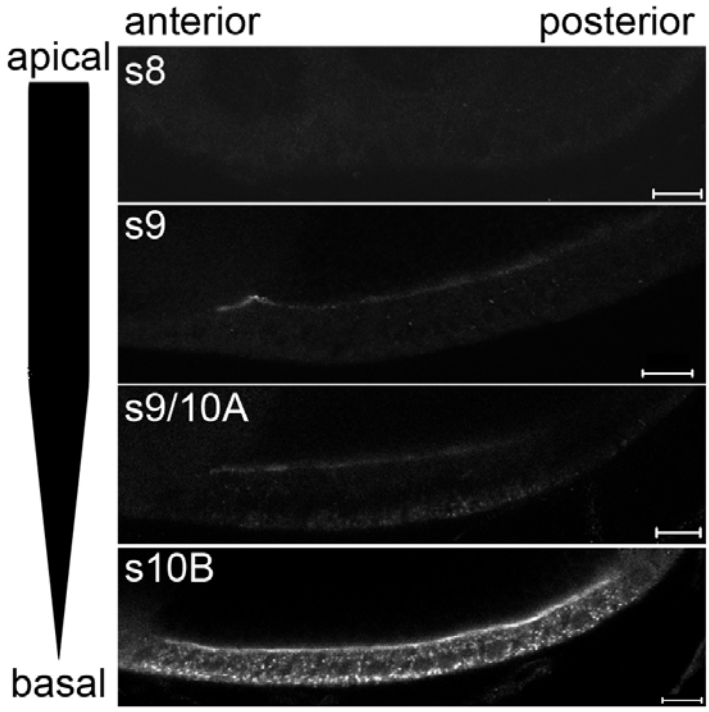

Fig. S2. The VM32E expression pattern during stages 8-10B of oogenesis. Posterior is towards the right. VM32E (white). Scale bars: 10 μm

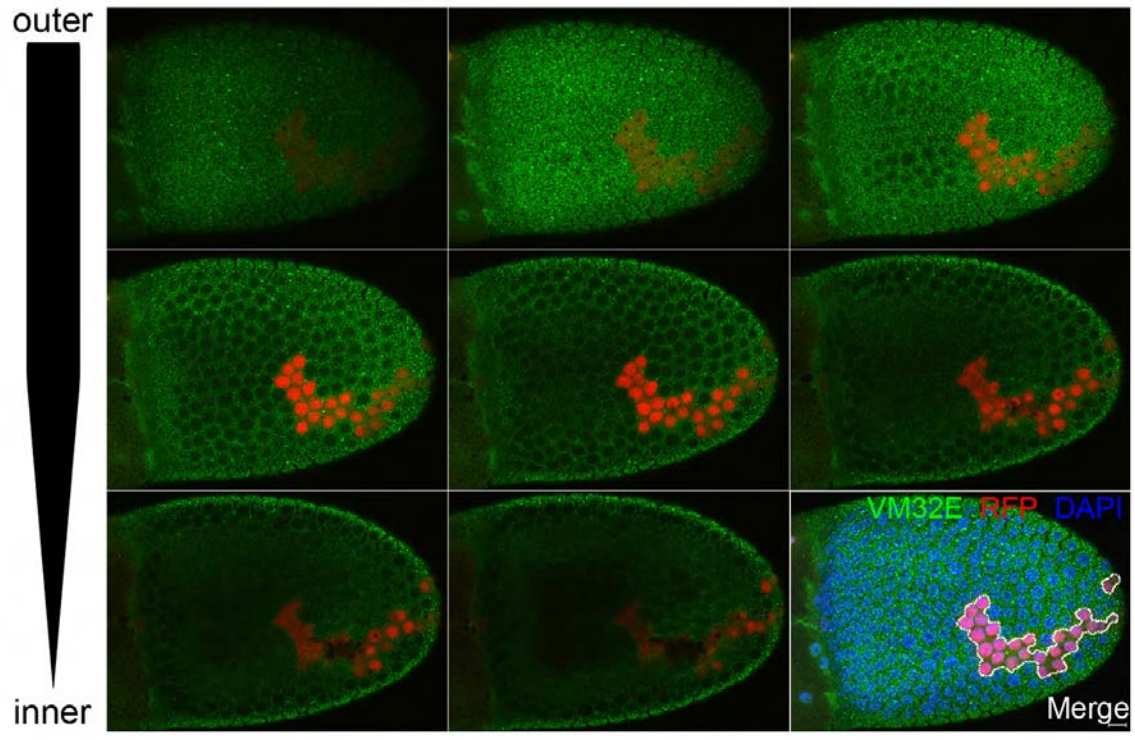

Fig. S3. A gallery of sectional images that were used to project Fig. 6B. Posterior is towards the right. VM32E, green; clone cells, red. Scale bars: 10 μm

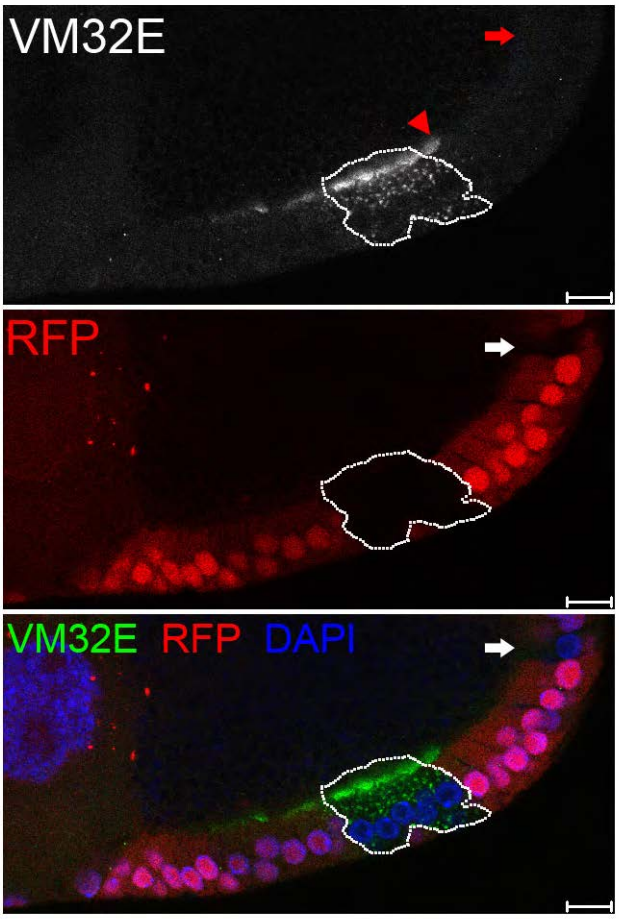

Fig. S4. A larger area of the egg chamber that contains the cropped image area Fig. 6C. This is a different section from the one shown in Fig. 6C. In addition to increased VM32E expression (green) in *miR-7* mutant cells (lack of RFP, outlined), high levels of VM32E appear to be diffused onto the surface of an adjacent wild-type cell (arrowhead). Posterior is towards the right. DAPI (blue) was used to mark cell nuclei. Scale bars: 10 µm

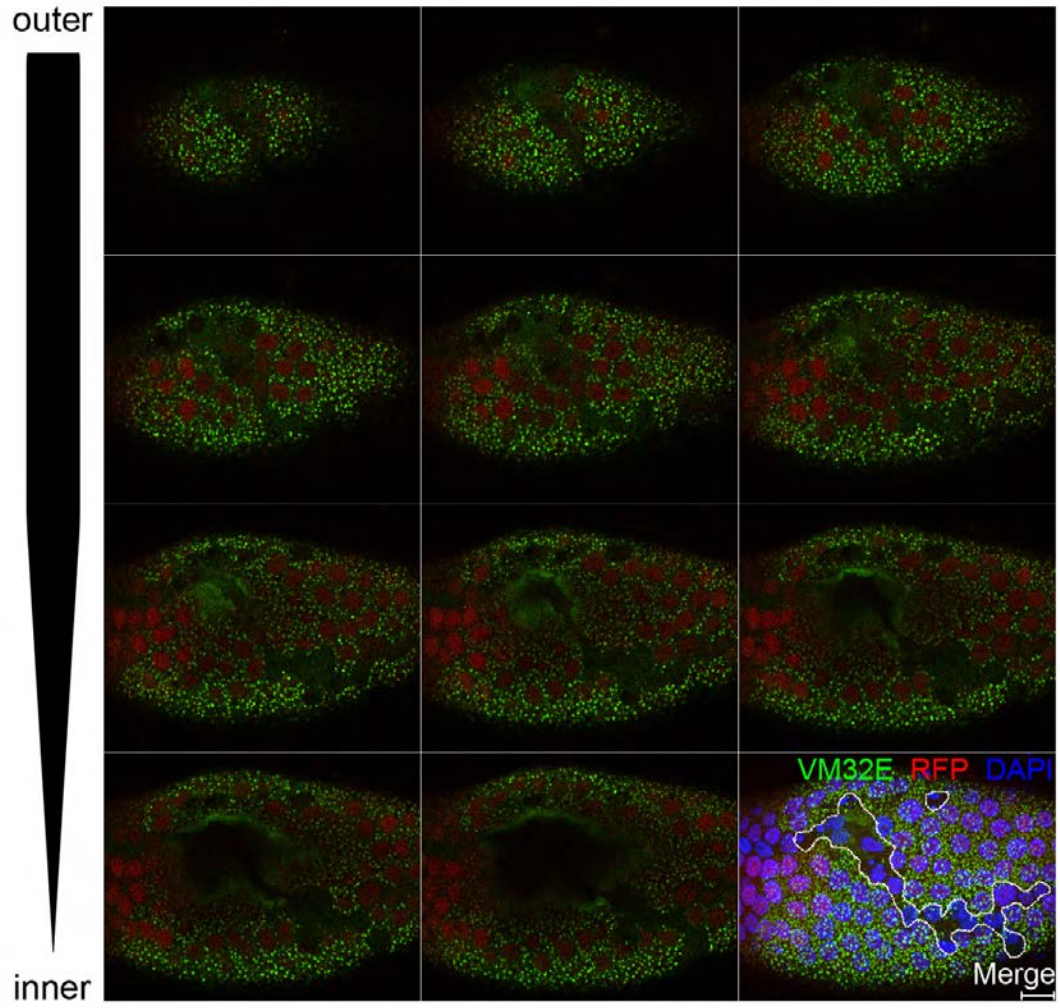

Fig. S5. A gallery of sectional images used to project Fig. 6E. Top and left panel is the outer layer. Posterior is towards the right. VM32E , green; clone cells, red. Scale bars: 10 μm

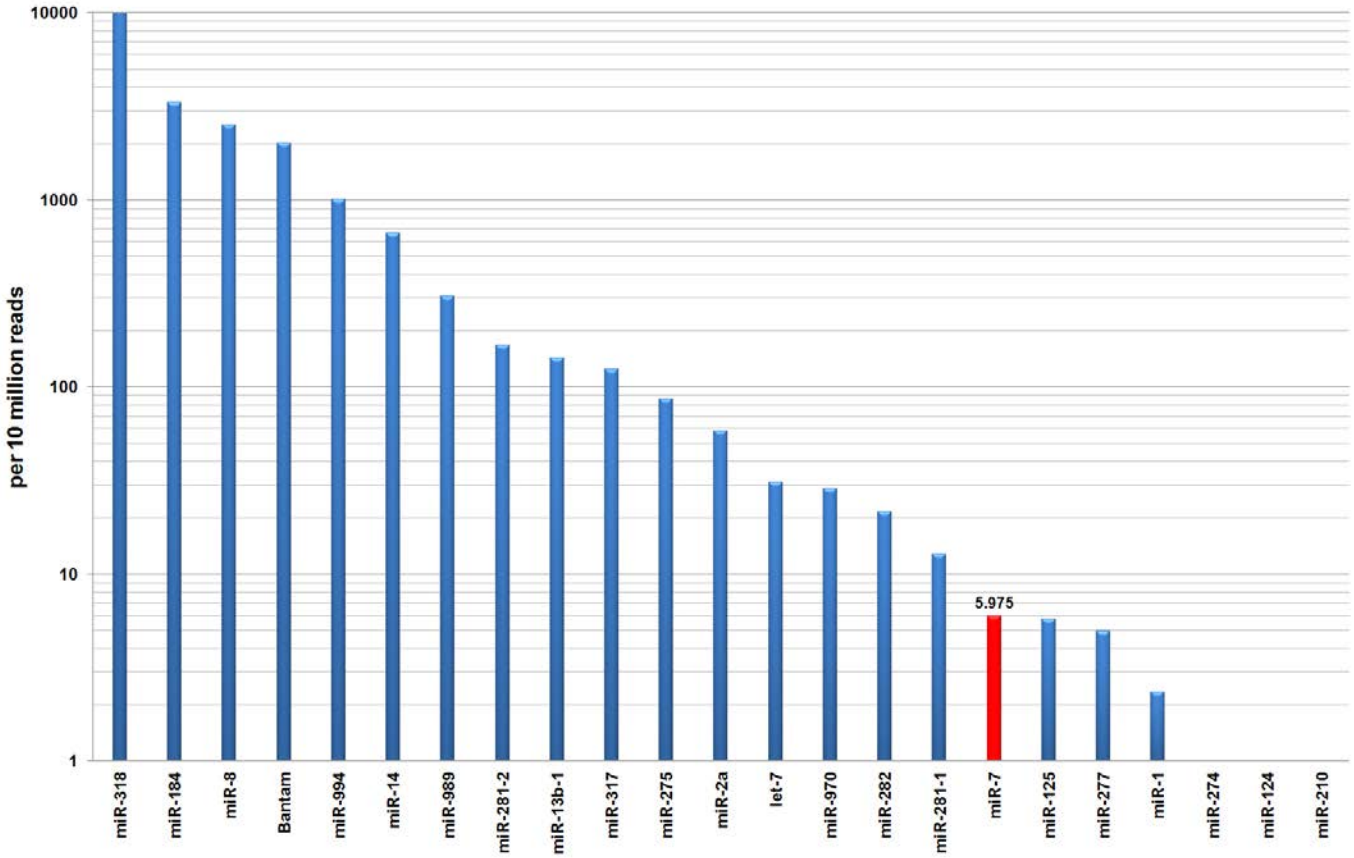

Fig. S6. Graphical results of relative expression levels of selected miRNAs in *w*^{1118} ovaries based on our RNA-seq analysis. Total RNA was isolated from *w*^{1118} ovaries by using the TRIzol reagent. Preparation of small RNA libraries was then carried out using the TreSeq small RNA preparation kit (Illumina) following the manufacturer's guide. Small RNA libraries (2 nM) were then sequenced on Illumina HiSeq 2000 system. Reads were demultiplexed and indexes removed with CASAVA v1.8.2 (Illumina). The 3′ adapter sequences were trimmed and reads with more than 10% containing a Sanger quality score of less than 25 were discarded with the FastX-toolkit (http://hannonlab.cshl.edu/fastx_toolkit/). We aligned the resulting reads to the FlyBase *Drosophila melanogaster* release 5.45 genome assembly (McQuilton et al., 2012) with Bowtie2 (Langmead and Salzberg, 2012) using default parameters. The per-base coverage was calculated per 10 million raw reads with BEDTools (Quinlan and Hall, 2010). The average coverage of two biological samples were used in subsequent data analysis. Different miRNAs are expressed at different levels in *Drosophila* ovaries. Among them, *miR-7* is expressed (read bar), but at a relatively low level. The *y*-axis shows the reads of each miRNA pre 10 million reads of total small RNA sequencing.